The application of computational chemistry & chemometrics to developing a method for online monitoring of polymer degradation in the manufacture of bioresorbable medical implants

Darren A. Whitaker[1], Fraser Buchanan[2], Domhnall Lennon[2], Mark Billham[2], Marion McAfee[1]

[1] Centre for Precision Engineering, Materials & Manufacturing, Institute of Technology Sligo, Sligo, Ireland
[2]School of Mechanical & Aerospace Engineering, Queen's University Belfast, Belfast, UK

Abstract. Bioresorbable polymers such as PLA have an important role to play in the development of temporary implantable medical devices with significant benefits over traditional therapies. However, development of new devices is hindered by high manufacturing costs associated with difficulties in processing the material. A major problem is the lack of insight on material degradation during processing. In this work, a method of quantifying degradation of PLA using IR spectroscopy coupled with computational chemistry and chemometric modeling is examined. It is shown that the method can predict the quantity of degradation products in solid-state samples with reasonably good accuracy, indicating the potential to adapt the method to developing an on-line sensor for monitoring PLA degradation in real-time during processing.

Keywords: Bioresorbable polymer, PLA, IR spectroscopy, computational chemistry, chemometrics

1 Introduction

Bioresorbable polymers are predicted to have a significant impact on modern medicine. They are increasingly being used to create temporary medical devices for implantation inside the human body. Such a device provides temporary mechanical support and/or other functions and break down over time into simple non-toxic products – ideally at the same rate that the body's own tissue regenerates. Drug-eluting bioresorbable medical implants are active implants that induce healing effects, in addition to their regular task of support. This effect is achieved by controlled release of active pharmaceutical ingredients (API) into the surrounding tissue as the polymer degrades.

The concept is being used or developed in a wide range of applications such as orthopaedics (fracture fixation plates, pins and screws, bone augmentation); surgery (ligament repair, wound closure sutures, suture anchors, skin staples, adhesion

barriers, drug delivery, antineoplastic delivery, ligating clips, hemostasis clips); stents, and tissue engineering.

However, high development and manufacturing costs have hindered growth of the industry. Bioresorbable polymers have a high cost and are difficult to process into the form required for the implant application. Usually some form of melt processing such as extrusion or injection molding is required, where the heating and shearing of the material tends to degrade the material. Currently, long and expensive trial and error periods are required to establish process settings for a new device and yet result in typical scrap rates of 25-30% - in many cases this is prohibitive to successful commercialisation. A major problem is the lack of information on key product properties during processing. Conventional polymer melt processing instrumentation consists largely of temperature and pressure sensors which give little insight on chemical changes to the material and are difficult to correlate to final product properties such as mechanical properties and biodegradation. Therefore, determination of product quality generally requires expensive and time-consuming off-line testing, resulting in long lead times and high rates of out of specification product.

In this work, the potential to use vibrational spectroscopy techniques together with chemometric modelling to analyse the degradation of a bioresorbable polymer is investigated. Such a method has the advantage of being possible to implement online during processing of the polymer and as such could provide real-time information on key product properties.

The remainder of the manuscript is organized as follows: first, a brief review is given of the effect of melt processing on the properties of PLA. Next the experimental thermal processing and characterization methods are described, followed by the computational chemistry techniques used to predict changes in the infra-Red (IR) spectra of the material when it undergoes degradation. This is followed by a description of the chemometric methods applied to develop a model relating polymer degradation to the experimentally acquired spectral data. The results are presented and discussed and finally some conclusions are posed on the future potential of the method to the manufacturing of bioresorbable medical devices.

2 Melt processing of bioresorbable polymers

Melt processing steps, particularly extrusion or injection molding, are the most common techniques for the forming of bioresorbable polymers such as Polylactic Acid (PLA) into final products. PLA is susceptible to thermal degradation and it is suggested that the temperatures, and residence times should be kept low to avoid reduction of polymer molecular weight and the formation of monomers[1]. The generation of monomers (lactide) during processing accelerates hydrolytic degradation of the material and has a significant impact on the biodegradation rate and rate of loss of mechanical properties. It has been found that increasing shear can

avoid the formation of monomer in the process [2, 3]. The processing of bioresorbables is significantly more complex than that of conventional engineering plastics, not only due to the sensitivity to degradation, but also since it is almost impossible to use fillers or additives to aid processing since most of these are not approved for use in the human body. Further, the high sensitivity of the materials to processing factors can mean that the slight variations between batches of raw material can result in significant product deviations under the same processing conditions. Adjusting the process settings to compensate for the feed variations is not an easy task as 1) the properties of the feed material are not accurately known; and 2) the key resulting properties of the polymer melt cannot be determined online during processing.
In the next sections the ability to analyse thermal degradation – encompassing changes in Molecular weight and/or lactide content – using a vibrational spectroscopy method which can then be applied in process, is examined.

3 Experimental Section

Sample Preparation

Poly-L-Lactide (PLLA) (Purasorb (PL38) (Purac, Gorinchem, The Netherlands) samples were produced by compression moulding. Pellets were placed in the centre of a stainless steel frame with internal dimensions of 100 x 60 mm. Before compression was started, a sheet of parchment paper was placed above and below the frame which was then sandwiched between two plates of stainless steel, before being placed into the press. This was to ensure the material did not come into direct contact with the press. Pellets were compression moulded at a range of temperatures with different residence times (Table 1). All samples were held at a pressure of 10MPa to produce flat sheets at 1 ± 0.1 mm thickness.

Table 1. Parameters of processing for PLA samples

Sample	Temperature (°C)	Time (min)	Cooling Method	Notes
A	200	10	Crash Cooled	Annealed
B	200	10	Crash Cooled	
C	220	10	Crash Cooled	
D	240	10	Crash Cooled	
E	240	30	Slow Cooled	

Infrared Spectroscopy

Infrared spectra of the PLA samples were recorded on a Perkin-Elmer spectrum 100 using an ATR sampling accessory. The spectra were recorded over a wavenumber range of 600 – 4000 cm^{-1}, with a resolution of 4cm^{-1}. A single spectrum was constructed from co-addition of 16 scans over the defined wavenumber range. Ten spectra were recorded from different places on the sample to account for any in sample variation which may be observed.

GC-MS

Gas Chromatography – Mass Spectrometry (GCMS) was carried out to quantify the lactide concentration in the PLLA samples.

A portion of the processed PLLA sample (*ca.* 1g) was dissolved in chloroform (18 mL). 2,4-dimethyl-gamma-pyrone (1 mL, 10,000 ppm) solution was added. A portion of this solution (1 mL) was added to a mixture of acetone (3 mL) and cyclohexane (16 mL). This solution was filtered using a 0.45 μm syringe filter and presented for GC analysis.

Samples were run on a Varian 3900 gas chromatograph fitted with an Agilent DB-FFAP column coupled to a Varian Saturn 2100T mass spectrometer. 1μL of the sample was injected into the injector port operating in splitless mode at 200 °C, the column oven was set at 65°C for 1 minute and then ramped at 30 °C · min^{-1} to 250 °C where the temperature was held for 2 minutes. After 1 minute the split valve of the injector was operated to purge the injector port of any residual sample. Carrier gas used was helium at a continuous flow rate of 0.8 mL · min^{-1}. Quantification was achieved by calculation of the relative response factors from a stock solution of lactide (10,000 ppm) and the internal standard (2,6-dimethyl-gamma-pyrone, 10,000 ppm).

Computational Chemistry

Ab Initio calculations were performed using the GAMESS[4] suite of programs and utilizing the computational power of ICHEC's FIONN supercomputer. Calculations were typically carried out on two of FIONNs nodes (each node containing 2 x 12 Intel Ivy Bridge cores and 64 GB of RAM).

Calculations were carried out for; *r,r-* (or D-), *s,s-* (or L-) and meso-lactide and also for a PLA 3-mer (Figure 1). The three isomers of lactide (*r,r-, s,s-* and *meso-*) were calculated separately to identify any band contributions which may be assigned to the presence of a specific isomer. This is important as all three isomers may be present within the sample, so any quantification will need to take into account contributions from all three isomers.

Calculations were performed at the B3LYP level of theory using the correlation consistent polarized valence double-zeta basis set (CC-PVDZ) proposed by Dunning *et al*[5, 6]. The work flow consisted of three steps: first the geometry was optimized; second a hessian calculation was carried out to compute IR frequencies and to ensure that the optimized geometry was a stable configuration (no negative frequencies); thirdly a Raman calculation was carried out using the geometry and hessian from the second calculation.

Following this, a VSCF (at B3LYP and CC-PVDZ) calculation was carried out to treat the anharmonicity of the vibrational modes.

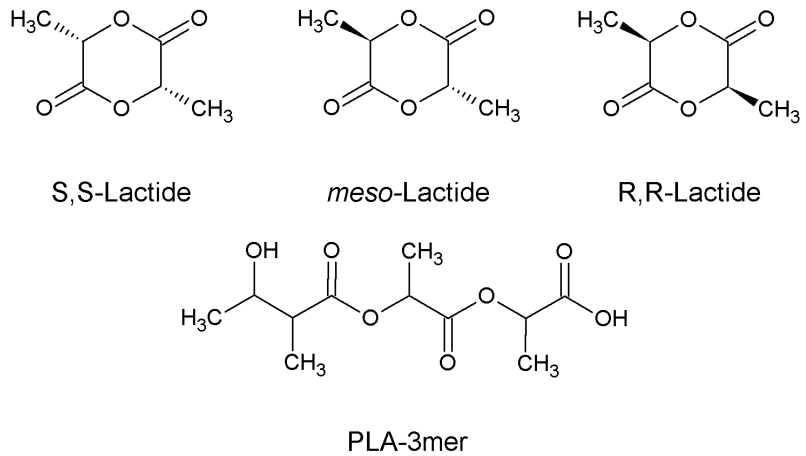

Figure 1. Molecular structures of lactide isomers and a PLA trimer

Spectral curves were constructed by adding a Lorentzian peak shape with a full width half maximum (FWHM) of 10-15 cm^{-1} to each transition, the sum of all the peaks were then calculated to display the computed trace[7, 8].

Chemometrics

Chemometrics were carried out using the R software[9] and RStudio as a graphical front end[10]. Linear discriminant analysis was carried out using the lda routine in the MASS package for R[11]. Data files were batch imported using custom written import routines. The aim of the chemometric analysis was to create a model which can classify the spectra based on the amount of degradation, or a model which can quantify the amount of lactide in the sample.

4 Results and Discussion

The optimised structures (Figure 2) for the s,s-, and r,r-lactide molecules show a "chair" like conformation with both CH_3 groups adopting an axial position, whereas in the r,s-lactide one CH_3 group locates at the axial and the other at the equatorial position. Bond lengths (not shown) for the r,r-(or s,s) and r,s-lactide molecules are in agreement with published *X*-Ray data[12].

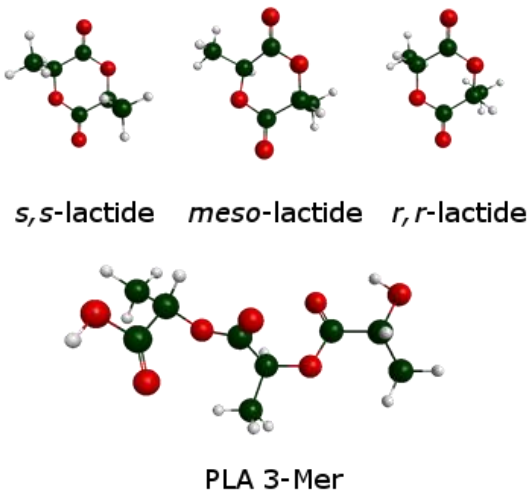

Figure 2. Optimised structures of lactide isomers and a PLA trimer

As would be expected the calculated IR spectra of r,r- and s,s- lactide are identical, the spectrum of r,s-lactide however, differs slightly (Figure 3). The main differences are observed in modes relating to CH vibrations, this is due to the variation in local environments of the methyl groups. For example the *r,r*- and *s,s*-lactides show a single transition for the $\nu_{(sym)}CH_3$ and the $\nu_{(asym)}CH_3$ whereas the *r,s*-lactide shows two transitions for each mode, clearly due to the non-symmetric nature of the *r.s*-lactide molecule (Figure 4).

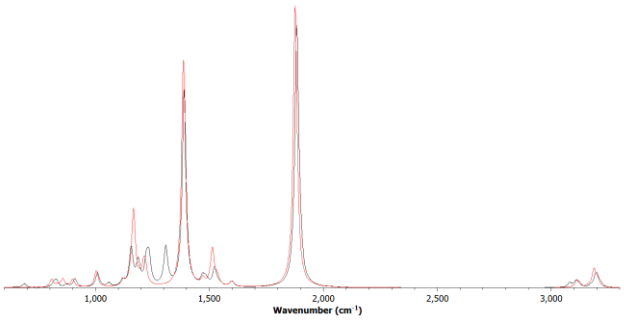

Figure 3. Predicted IR spectrum of *meso*- (black) and *r,r-/s,s*-Lactide (red)

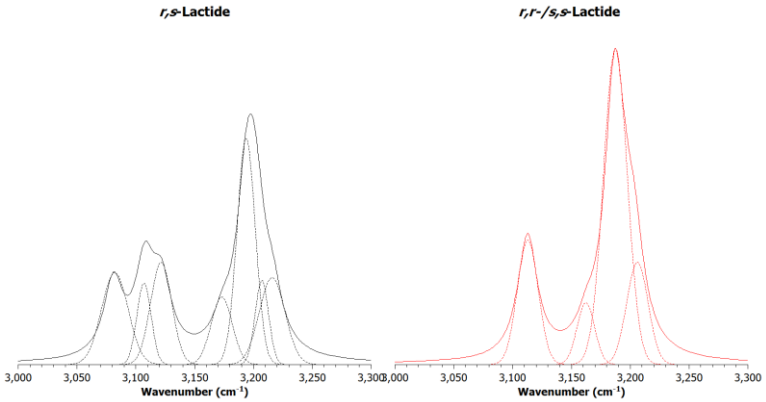

Figure 4. CH stretching region of predicted spectra of lactide isomers displaying fitted peaks under curves (dotted)

These predictions display a relatively good agreement with experimental values (Figure 5) deviations are expected as the homochiral racemic sample is likely to contain small amounts of the heterochiral isomer (due to epimerisation during storage) which would result in peak broadening and shifting.

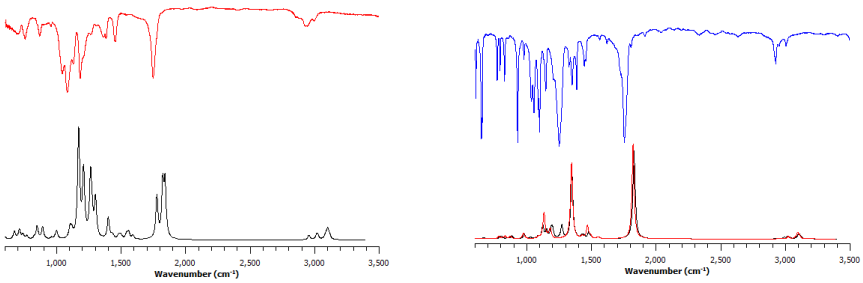

Figure 5. Predicted (bottom) and experimental (top) spectra for a PLA trimer (left) and the lactide isomers (right)

Chemometric analysis showed a reasonable separation between samples, which allowed classification boundaries to be observed. PCA was performed to reduce the dimensionality of the data, from this LDA was performed on the first 10 components. A plot of LD1 vs LD2 as a result of this shows clear separation between the samples. Sample A (Figure 6, black points) was located the furthest away from the main cluster, this is likely owing to the difference in optical properties of this sample from the annealing process. Samples B, C, D, and E were clustered with minimal variation in LD1 but good separation from LD2. Two spectra of each sample were run through the model and all but two were correctly classified (Figure 6, filled circles)

Following a good separation, two quantitative models based on PLS analysis was built. One model used the whole spectrum and another focused on just the CH

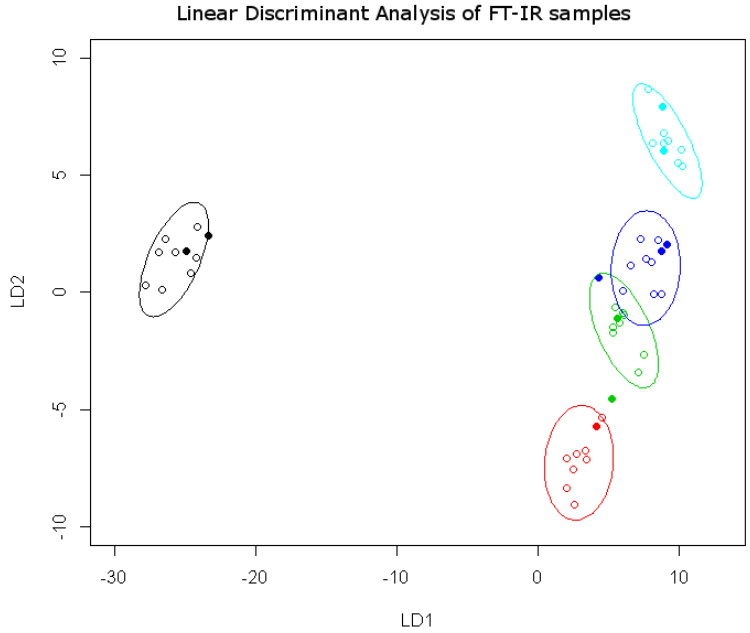

Figure 6. LD1 vs LD2 for the IR spectra of processed PLA samples

stretching region (as computations suggested variation would be seen here from increasing CH contributions from lactide as concentrations increased). GCMS results allowed quantification of lactide content in the processed samples (Table 2), these values were used to construct a model trained with a 30 spectra subset of the data (5 spectra from each sample) and then tested with the same sized subset. The

Table 2. Lactide content of samples

Sample	Lactide (w/w %)
A	0.12
B	0.07
C	0.09
D	0.24
E	1.20

model was able to predict the actual lactide content to within <±5 % in most cases, although some outliers were greater than this (Table 3). Overall performance (measured using the RMSEP values) of the model using just the CH stretching frequencies was better than the model using the full spectrum (Figure 7).

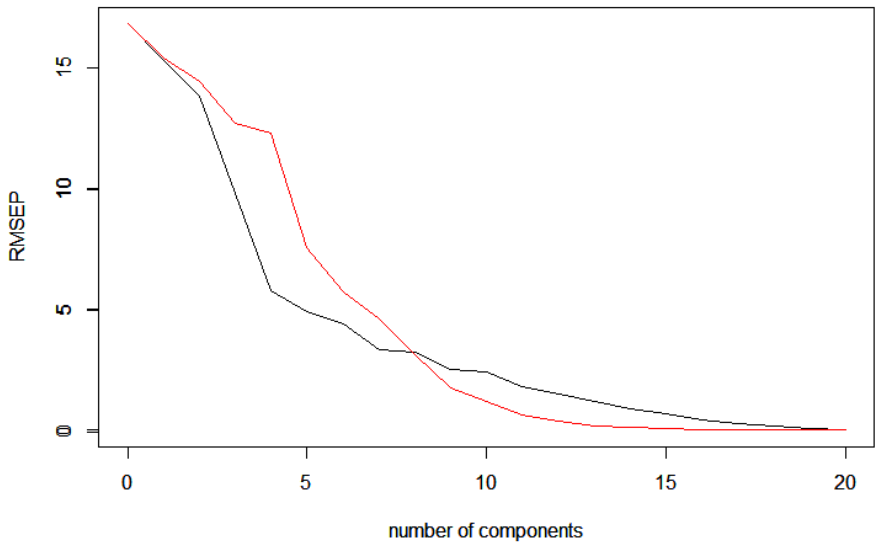

Figure 7. RMSEP values for the PLS model. Model using whole spectrum (black) and model using CH stretching region only (red).

5 Conclusions

The initial work presented in this paper has centered on the construction of models which were able to classify PLA samples showing differing degrees of process induced degradation. This was extended to build a model which was able to predict the lactide content of the analysed sample with a relatively good degree of accuracy. The computational methodology employed was able to identify areas of the spectrum where sufficient variation due to process induced lactide may exist. When compared with a whole spectrum approach this significantly improved the predictive accuracy of the model

There are still improvements to be made, these are based on an improvement of data acquisition and an increase in data points / data classes made available for training the models. Additionally the models will be extended for use with other techniques which are perhaps more conducive to online monitoring (nIR and Raman spectroscopies), with the overall goal being a system which updates the user in real time which class the sample belongs to, with the possibility of providing an estimated lactide content.

Table 3. Actual and predicted values from the PLS models

	CH Stretching Region Model		Whole Spectrum Model	
Lactide concentration	Predicted Concentration	Δ	Predicted Concentration	Δ
0.12	0.26	0.14	0.12	0.00
0.12	0.44	0.32	0.22	0.10
0.12	0.19	0.07	0.06	-0.06
0.12	0.18	0.06	-0.01	-0.13
0.12	0.16	0.04	0.15	0.03
0.07	-0.20	-0.27	0.01	-0.06
0.07	-0.09	-0.16	0.07	0.00
0.07	0.00	-0.07	0.06	-0.01
0.07	-0.08	-0.15	0.16	0.09
0.07	0.36	0.29	0.26	0.19
0.09	0.46	0.37	0.27	0.18
0.09	0.25	0.16	0.17	0.08
0.09	0.32	0.23	0.25	0.16
0.09	0.10	0.01	0.02	-0.07
0.09	0.09	0.00	0.13	0.04
0.24	0.08	-0.16	0.17	-0.07
0.24	0.21	-0.03	0.25	0.01
0.24	0.21	-0.03	0.21	-0.03
0.24	0.03	-0.21	0.05	-0.19
0.24	0.54	0.30	0.34	0.10
1.20	0.97	-0.23	0.93	-0.27
1.20	0.97	-0.23	0.92	-0.28
1.20	1.25	0.05	1.19	-0.01
1.20	1.19	-0.01	1.12	-0.08
1.20	1.07	-0.13	1.12	-0.08
0.12	0.26	0.14	0.12	0.00
0.12	0.44	0.32	0.22	0.10
0.12	0.19	0.07	0.06	-0.06
0.12	0.18	0.06	-0.01	-0.13
0.12	0.16	0.04	0.15	0.03

Acknowledgements

The research leading to these results has received funding from the European Union's Seventh Framework Programme managed by REA-Research Executive Agency http://ec.europa.eu/research/rea(FP7/2007-2013) under grant agreement n°605086 FP7-SME-2012. The Science Foundation Ireland (SFI) and Higher Education Authority funded Irish Centre for High End Computing (ICHEC) is acknowledged for access to computational facilities.

6 References

1. Taubner, V., Shishoo, R.: Influence of processing parameters on the degradation of poly(L-lactide) during extrusion. J. Appl. Polym. Sci. 79, 2128–2135 (2001).

2. Paakinaho, K., Ellä, V., Syrjälä, S., Kellomäki, M.: Melt spinning of poly(l/d)lactide 96/4: Effects of molecular weight and melt processing on hydrolytic degradation. Polym. Degrad. Stab. 94, 438–442 (2009).

3. Ellä, V., Nikkola, L., Kellomäki, M.: Process-induced monomer on a medical-grade polymer and its effect on short-term hydrolytic degradation. J. Appl. Polym. Sci. 119, 2996–3003 (2011).

4. Schmidt, M.W., Baldridge, K.K., Boatz, J.A., Elbert, S.T., Gordon, M.S., Jensen, J.H., Koseki, S., Matsunaga, N., Nguyen, K.A., Su, S., Windus, T.L., Dupuis, M., Montgomery, J.A.: General atomic and molecular electronic structure system. J. Comput. Chem. 14, 1347–1363 (1993).

5. Dunning, T.H.: Gaussian basis sets for use in correlated molecular calculations. I. The atoms boron through neon and hydrogen. J. Chem. Phys. 90, 1007 (1989).

6. Kendall, R.A., Dunning, T.H., Harrison, R.J.: Electron affinities of the first-row atoms revisited. Systematic basis sets and wave functions. J. Chem. Phys. 96, 6796 (1992).

7. Brauer, B., Pincu, M., Buch, V., Bar, I., Simons, J.P., Gerber, R.B.: Vibrational spectra of α-glucose, β-glucose, and sucrose: anharmonic calculations and experiment. J. Phys. Chem. A. 115, 5859–72 (2011).

8. Pele, L., Šebek, J., Potma, E.O., Benny Gerber, R.: Raman and IR spectra of butane: Anharmonic calculations and interpretation of room temperature spectra. Chem. Phys. Lett. 515, 7–12 (2011).

9. R Core Team: R: A Language for Statistical Computing. R Found. Stat. Comput. (2013).

10. RStudio: RStudio: Intergrated Development Environment for R, (2013).

11. Venables, W.. N., Ripley, B.D.: Modern Applied Statistics with S. Springer, New York (2002).

12. Van Hummel, G.J., Harkema, S., Kohn, F.E., Feijen, J.: Structure of 3,6-dimethyl-1,4-dioxane-2,5-dione [D-,D-(L-,L-)lactide]. Acta Crystallogr. Sect. B Struct. Crystallogr. Cryst. Chem. 38, 1679–1681 (1982).